Clinical Cancer Research

ERCC2 Helicase Domain Mutations Confer Nucleotide Excision Repair Deficiency and Drive Cisplatin Sensitivity in Muscle-Invasive Bladder Cancer

Qiang Li[1,2], Alexis W. Damish[3], Zoë Frazier[3], David Liu[4,5,6], Elizaveta Reznichenko[3,7], Atanas Kamburov[5,8], Andrew Bell[9], Huiyong Zhao[9], Emmet J. Jordan[10], S. Paul Gao[10], Jennifer Ma[9], Philip H. Abbosh[11,12], Joaquim Bellmunt[4], Elizabeth R. Plimack[13], Jean-Bernard Lazaro[3,7], David B. Solit[10,14,15], Dean Bajorin[14], Jonathan E. Rosenberg[14], Alan D. D'Andrea[3,7,16], Nadeem Riaz[9], Eliezer M. Van Allen[4,5], Gopa Iyer[14], and Kent W. Mouw[3,16]

Abstract

Purpose: DNA-damaging agents comprise the backbone of systemic treatment for many tumor types; however, few reliable predictive biomarkers are available to guide use of these agents. In muscle-invasive bladder cancer (MIBC), cisplatin-based chemotherapy improves survival, yet response varies widely among patients. Here, we sought to define the role of the nucleotide excision repair (NER) gene *ERCC2* as a biomarker predictive of response to cisplatin in MIBC.

Experimental Design: Somatic missense mutations in *ERCC2* are associated with improved response to cisplatin-based chemotherapy; however, clinically identified *ERCC2* mutations are distributed throughout the gene, and the impact of individual *ERCC2* variants on NER capacity and cisplatin sensitivity is unknown. We developed a microscopy-based NER assay to profile *ERCC2* mutations observed retrospectively in prior studies and prospectively within the context of an institution-wide tumor profiling initiative. In addition, we created the first *ERCC2*-deficient bladder cancer preclinical model for studying the impact of *ERCC2* loss of function.

Results: We used our functional assay to test the NER capacity of clinically observed *ERCC2* mutations and found that most *ERCC2* helicase domain mutations cannot support NER. Furthermore, we show that introducing an *ERCC2* mutation into a bladder cancer cell line abrogates NER activity and is sufficient to drive cisplatin sensitivity in an orthotopic xenograft model.

Conclusions: Our data support a direct role for *ERCC2* mutations in driving cisplatin response, define the functional landscape of *ERCC2* mutations in bladder cancer, and provide an opportunity to apply combined genomic and functional approaches to prospectively guide therapy decisions in bladder cancer.

See related commentary by Grivas, p. 907

Introduction

Large-scale genomic studies have identified thousands of somatic mutations across dozens of tumor types (1, 2). However, with the exception of a few well-studied cancer genes, the impact of these mutations on protein function and cellular phenotypes including drug sensitivity has not been systematically tested. With the rapid adoption of prospective tumor genomic profiling, there is now greater urgency to provide clinicians and patients with insight into the clinical significance of not only highly recurrent genomic variants but also non-hotspot mutations that reside within the long tail of the frequency distribution (3). For genes with numerous potentially actionable rare variants, efficient and reliable cellular assays are needed to determine the functional impact of large numbers of tumor-associated mutations.

[1]Department of Surgery, Urology Service, Memorial Sloan Kettering Cancer Center, New York, New York. [2]Department of Urology, Roswell Park Cancer Institute, Buffalo, New York. [3]Department of Radiation Oncology, Dana-Farber Cancer Institute/Brigham and Women's Hospital, Boston, Massachusetts. [4]Department of Medical Oncology, Dana-Farber Cancer Institute, Boston, Massachusetts. [5]Broad Institute of Harvard and MIT, Cambridge, Massachusetts. [6]Cancer Center, Massachusetts General Hospital, Boston, Massachusetts. [7]Center for DNA Damage and Repair, Dana-Farber Cancer Institute, Boston, Massachusetts. [8]Drug Discovery, Bayer AG, Berlin, Germany. [9]Department of Radiation Oncology, Memorial Sloan Kettering Cancer Center, New York, New York. [10]Human Oncology and Pathogenesis Program, Memorial Sloan Kettering Cancer Center, New York, New York. [11]Molecular Therapeutics Program, Fox Chase Cancer Center, Philadelphia, Pennsylvania. [12]Department of Urology, Einstein Medical Center, Philadelphia, Pennsylvania. [13]Department of Hematology/Oncology, Fox Chase Cancer Center, Philadelphia, Pennsylvania. [14]Genitourinary Oncology Service, Department of Medicine, Memorial Sloan Kettering Cancer Center, New York, New York. [15]Weill Cornell Medical College, Cornell University, New York, New York. [16]Ludwig Center at Harvard, Boston, Massachusetts.

Note: Supplementary data for this article are available at Clinical Cancer Research Online (http://clincancerres.aacrjournals.org/).

Q. Li, A.W. Damish, and Z. Frazier share first authorship.

N. Riaz, E.M. Van Allen, G. Iyer, and K.W. Mouw share senior authorship.

Corresponding Authors: Kent W. Mouw, Brigham and Women's Hospital/Dana-Farber Cancer Institute, 450 Brookline Avenue, HIM 350, Boston, MA 02215. Phone: 617-582-9355; Fax: 617-582-8213; E-mail: kent_mouw@dfci.harvard.edu; and Gopa Iyer, Memorial Sloan Kettering Cancer Center, 300 East 66th Street, BAIC 1259, New York, NY 10065. Phone: 646-422-4362; E-mail: iyerg@mskcc.org

doi: 10.1158/1078-0432.CCR-18-1001

Translational Relevance

Mutations in DNA repair genes can have important therapeutic implications, but determining the functional impact of novel mutations is challenging. In bladder cancer, missense mutations in the nucleotide excision repair (NER) gene *ERCC2* are associated with improved response to cisplatin-based chemotherapy; however, mutations are distributed across the gene, and the functional impact of most individual *ERCC2* mutations is unknown. Here, we develop a microscopy-based assay to directly measure the NER capacity of clinically observed *ERCC2* mutations and find that most helicase domain mutations impair NER function. Furthermore, we develop a preclinical *ERCC2*-deficient bladder cancer model and show that *ERCC2* loss is sufficient to drive cisplatin sensitivity. These findings establish *ERCC2* as a predictive biomarker in bladder cancer and highlight the potential to combine genomic and functional approaches in a coclinical trial paradigm to guide precision oncology for conventional chemotherapy agents.

Cisplatin-based regimens are used in a wide range of malignancies and are a standard of care for patients with muscle-invasive or metastatic bladder cancer (MIBC; refs. 4, 5). However, there is significant variability in patient response to cisplatin, and given its significant toxicities, only a fraction of eligible patients receive cisplatin-based therapy (6). We previously identified an association between somatic *ERCC2* mutations and pathologic complete response to neoadjuvant cisplatin-based chemotherapy in MIBC (DFCI/MSK cohort; ref. 7), which was subsequently validated in an independent cohort (FCCC cohort; ref. 8). In both cohorts, patients with *ERCC2*-mutated tumors had improved overall survival compared to patients with *ERCC2* wild-type (WT) tumors. Furthermore, additional studies have demonstrated an association between mutations in DNA repair genes (including *ERCC2*) and response to DNA-damaging agents in metastatic bladder cancer (9), and recently, an association was also identified between DNA repair gene mutations and improved response to anti–PD-1/PD-L1 agents (10, 11).

ERCC2 is a DNA helicase and a member of the nucleotide excision repair (NER) pathway, which repairs intrastrand cross-links created by genotoxins such as UV irradiation and platinum chemotherapies (12). Functional analysis of a small subset of the somatic *ERCC2* missense mutations identified in the DFCI/MSK cohort showed that these mutations were unable to rescue the cisplatin or UV sensitivity of an *ERCC2*-deficient cell line, suggesting that they confer loss of cellular NER capacity (7). However, the functional and clinical significance of the majority of *ERCC2* mutations identified in MIBC cohorts are unknown, and reliable and efficient assays to directly measure the impact of mutations on cellular NER capacity are lacking. Moreover, the effect of *ERCC2* mutations on NER capacity has not been tested directly in bladder cancer cells, and the impact of *ERCC2* mutations on bladder tumor sensitivity to clinically relevant DNA repair–directed therapies such as platinum agents, ionizing radiation, and PARP inhibitors is unknown.

DNA repair mutations can have important implications for genomic stratification and management decisions, and functional analysis of DNA repair mutations across tumor types remains an important challenge (13, 14). To better understand the role of *ERCC2* mutations in bladder cancer, we performed NER profiling of *ERCC2* mutations and directly measured the impact of an *ERCC2* mutation on cisplatin sensitivity in a bladder cancer model. We find that nearly all clinically observed *ERCC2* mutations result in loss of cellular NER capacity and that an *ERCC2* mutation is sufficient to increase cisplatin sensitivity in bladder cancer cells. Together, these data strongly support a role for *ERCC2* mutations as a predictive biomarker in MIBC and illustrate the potential to combine functional and genomic assays for prospective profiling of bladder tumors to inform clinical decision-making.

Materials and Methods

Cohort characteristics and genomic analyses

A pan-cancer analysis of *ERCC2* mutations was performed by identifying all *ERCC2* missense mutations from an institutional analysis of 10,919 tumors (15). Subsequently, all *ERCC2* coding mutations in a pooled cohort of >1,500 tumors comprised of prospectively collected institutional samples as well as published The Cancer Genome Atlas (TCGA) and single institution series were identified and mapped to the *ERCC2* gene (Supplementary Table S1).

Somatic *ERCC2* mutations for functional analysis were identified from three independent published cohorts: the DFCI/MSK cohort (50 cases), the FCCC cohort (48 cases), and the TCGA cohort (130 cases). Cohort and mutation data are summarized in Supplementary Table S2.

In one case from the DFCI/MSK cohort, posttreatment tumor was analyzed and revealed an *ERCC2* E86Q mutation. This mutation was not originally called in the pretreatment tumor due to low number of reads, but subsequent manual review and phylogenetic analysis of the pre- and posttreatment tumors revealed the *ERCC2* E86Q mutation in the pretreatment biopsy in 1 of 7 reads (Supplementary Fig. S1; ref. 16).

Clonality of *ERCC2* mutations was determined by using ABSOLUTE to infer tumor purity (i.e., the percentage of DNA in the sample from the tumor vs. the stroma or infiltrating cells) and ploidy, then adjusting the observed variant allele fraction for the inferred purity and local copy number to generate a cancer cell fraction (CCF; the fraction of cancer cells inferred to contain the mutation; ref. 17). The mutation was inferred to be clonal when the 95% confidence interval for the inferred CCF included 1.0.

Cell lines and reagents

An SV40-transformed fibroblast cell line derived from a patient with xeroderma pigmentosum of genetic complementation group D (GM08207) was purchased from Coriell Institute (Camden, NJ) and was maintained in DMEM plus 10% FCS, 2 mmol/L L-glutamine, and 1% penicillin/streptomycin at 37°C and 5% CO_2. The cell line is a compound heterozygote harboring $ERCC2^{R683W}$ and $ERCC2^{\Delta 36\_61}$ alterations.

A Myc-DDK–tagged WT *ERCC2* lentiviral expression plasmid was purchased from Origene. Point mutations were introduced by site-directed mutagenesis using the QuikChange protocol (Qiagen), and all mutations were confirmed by Sanger sequencing. WT or mutant *ERCC2* plasmids were expanded in *E. coli* TOP10 cells (Invitrogen), purified using an Anion Exchange Kit

(Qiagen), and stably expressed in GM08207 cells by lentiviral infection (Supplementary Methods).

The KU 19-19 cell line was purchased from DSMZ and maintained in RPMI media supplemented 10% FCS, 2 mmol/L L-glutamine, and 1% penicillin/streptomycin at 37°C and 5% CO_2. The LentiCRISPR v2 plasmid was obtained from Addgene (catalog no. 52961; ref. 18). Oligonucleotides (GGCAACCTTCACCATGACGC) targeting the genomic DNA sequence around T484 of *ERCC2* were subcloned into this plasmid. Lentivirus was produced by transfecting the plasmid together with lentiviral packaging plasmids psPAX2 and pMD2.G (Addgene) into HEK293T cells. KU19-19 bladder cancer cells were infected and sorted into 96-well plate using FACS single-cell sorting. Single-cell clones were screened for ERCC2 protein expression by Western blot analysis and genotyped by genomic locus PCR and Sanger sequencing (PCR primers: forward: 5′-TGGGGTGTATTTTGGACTCAGATG; reverse: 5′-ACAGAGACGGAGACGGAGAGGAAG). The KE1 cell line (*T484Rfs*9*, *M483Rfs*10*, *M483*_T484del) was identified and confirmed using MSK-IMPACT.

DDB2 proteoprobe assay

The DDB2-FLAG-HA proteoprobe was purified from HeLa S3 cells as described previously (19). Briefly, cells were seeded on 24-well PTFE printed slides (Electron Microscopy Sciences) at a density of 3,500 cells per well. Cells were covered in 3 mL of DropArray Sealing Fluid (Curiox) and incubated overnight at 37°C. The following day, the slides were treated with 20 J using a UV-B irradiator (Strategene) or mock-irradiated. Five or 150 minutes following irradiation, slides were fixed with methanol and then serially rehydrated in PBS/methanol solutions. Wells were blocked with a 10% BSA in PBS, and then incubated for one hour at 37°C with the DDB2 proteoprobe in PBS-BSA solution. Wells were washed once with PBS and then incubated for one hour in a 10% BSA solution containing 1:200 rabbit anti-HA (Cell Signaling Technology) and 1:650 mouse anti-Myc (Cell Signaling

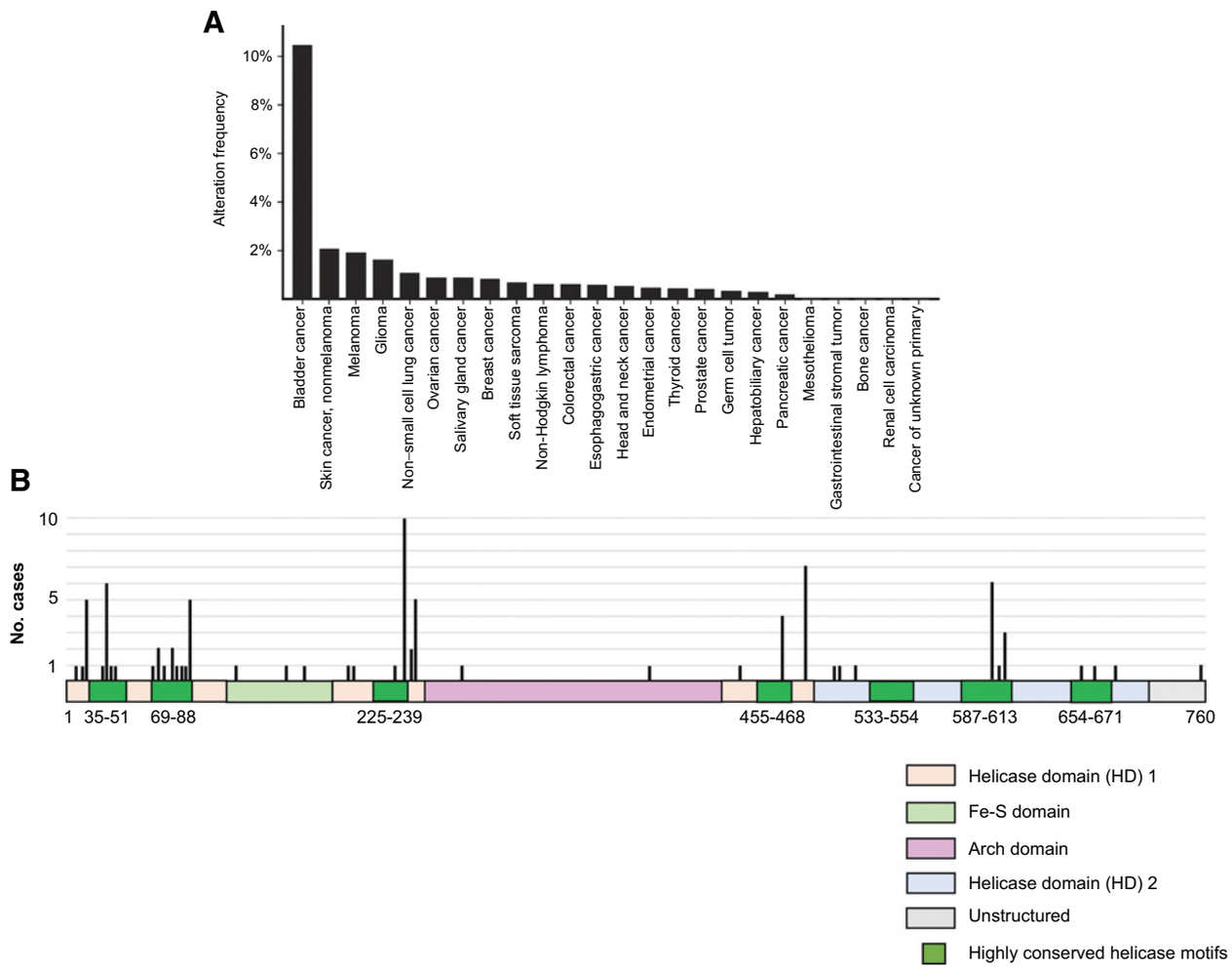

Figure 1.

Frequency and distribution of *ERCC2* mutations. **A,** Frequency of *ERCC2* mutations by tumor type across 10,919 tumors sequenced using MSK-IMPACT (15). Only tumor types with ≥100 samples are shown, and tumors with an MSI score ≥10 (i.e., hypermutated tumors) are excluded. **B,** Location of *ERCC2* mutations identified in published and ongoing prospective clinical cohorts.

Technology) primary antibodies. After washing, wells were incubated for one hour in a 10% BSA solution containing 1:300 dilutions of goat anti-mouse Alexa Fluor 488 IgG (Life Technologies) and goat anti-rabbit Alexa Fluor 594 IgG (Life Technologies) secondary antibodies. Cells were then washed twice with PBS and once with deionized water, then mounted using Fluoro-Gel II with DAPI (Electron Microscopy Sciences). Images were taken using an AxioCam MRM camera coupled with a 106/0.45 plan-Apochromat or 636/1.4 oil plan-Apochromat objective (Zeiss). Each well was photographed six times at five different focal points. The overlaid compilations were analyzed using the CellProfiler imaging platform (Broad Institute, Cambridge, MA), and manual counts (50 nuclei/well) were also performed. All experiments were performed in triplicate. DNA repair proficiency was quantified as the fraction of DDB2 foci repaired at 150 minutes.

Cell sensitivity assays

For cisplatin and other drug sensitivity assays, cells were transferred to 96-well plates at a density of 500 to 1,500 cells per well. The following day, cisplatin (or other drug) was serially diluted in media and added to the wells. After 72 to 96 hours, CellTiter-Glo (Promega) was added to the wells and the plates were scanned using a luminescence microplate reader (BioTek). Survival at each drug concentration was plotted as a percentage of survival in drug-free media, with error bars representing the SD of at least three experiments. See Supplementary Methods for details.

Xenograft studies

All animal work was done in accordance with a protocol approved by the MSKCC Institutional Animal Care and Use Committee. NSG female mice (The Jackson Laboratory) between 6 and 8 weeks of age were used for orthotopic studies. For real-time bioluminescent tracking and measuring, KU19-19 parental or KE1 *ERCC2*-mutant cells were labeled by a retroviral Firefly luciferase gene/GFP double-expressing reporter construct, SFG-FLuc-IRES2-GFP (20). A total of 1×10^5 labeled cells were resuspended in 10 μL of a 1:1 mixture of PBS and Matrigel (Corning) and injected orthotopically into the bladder muscle layer. Mice were imaged once per week with an In Vivo Imaging System (IVIS, Xenogen) with a collection time of 10 seconds. Tumor bioluminescence was quantified by integrating the photonic flux (photons/second) through a region encircling each tumor as determined by the LIVING IMAGES software package (Xenogen). Upon imaging, mice were randomized into 2 treatment groups (4 mice/group) and treated with either vehicle or cisplatin (3 mg/kg i.p.) once per week for 3 consecutive weeks. Mice were observed daily for signs of morbidity/mortality, and body weights were assessed twice weekly.

Results

ERCC2 is recurrently mutated in MIBC with mutations distributed across the gene

To understand the landscape of *ERCC2* mutations in cancer, we mapped the frequency of *ERCC2* mutations across tumor types. *ERCC2* has been previously identified as a recurrently mutated gene in bladder cancer (21), and we found that the frequency of *ERCC2* mutations was considerably higher in bladder cancer than in any other common solid tumor types (Fig. 1A). Next, we determined the distribution of clinically observed bladder tumor

Table 1. Summary of MIBC cohorts

Cohort	No. of cases	Clinical details	No. of patients with ERCC2 mutated tumor	Total no. of ERCC2 mutations	No. of unique ERCC2 mutations	Reference(s)
TCGA	130	No neoadjuvant therapy prior to cystectomy	16 (12%)	16	13	21
DFCI/MSK	50	Neoadjuvant cisplatin-based chemotherapy followed by cystectomy "Responder": pT0/pTis disease in cystectomy specimen ($n = 25$) "Nonresponder": ≥pT2 disease in cystectomy specimen ($n = 25$) (no patients had pTa/pT1 disease in cystectomy specimen)	10 (20%) (9/25 responders, 1/25 nonresponders)	10	9	7
FCCC	48	Neoadjuvant cisplatin-based chemotherapy followed by cystectomy "Responder": pT0/pTis/pTa disease in cystectomy specimen ($n = 20$) "Nonresponder": all others ($n = 28$)	10 (21%) (8/20 responders, 2/28 nonresponders)	11	10	8

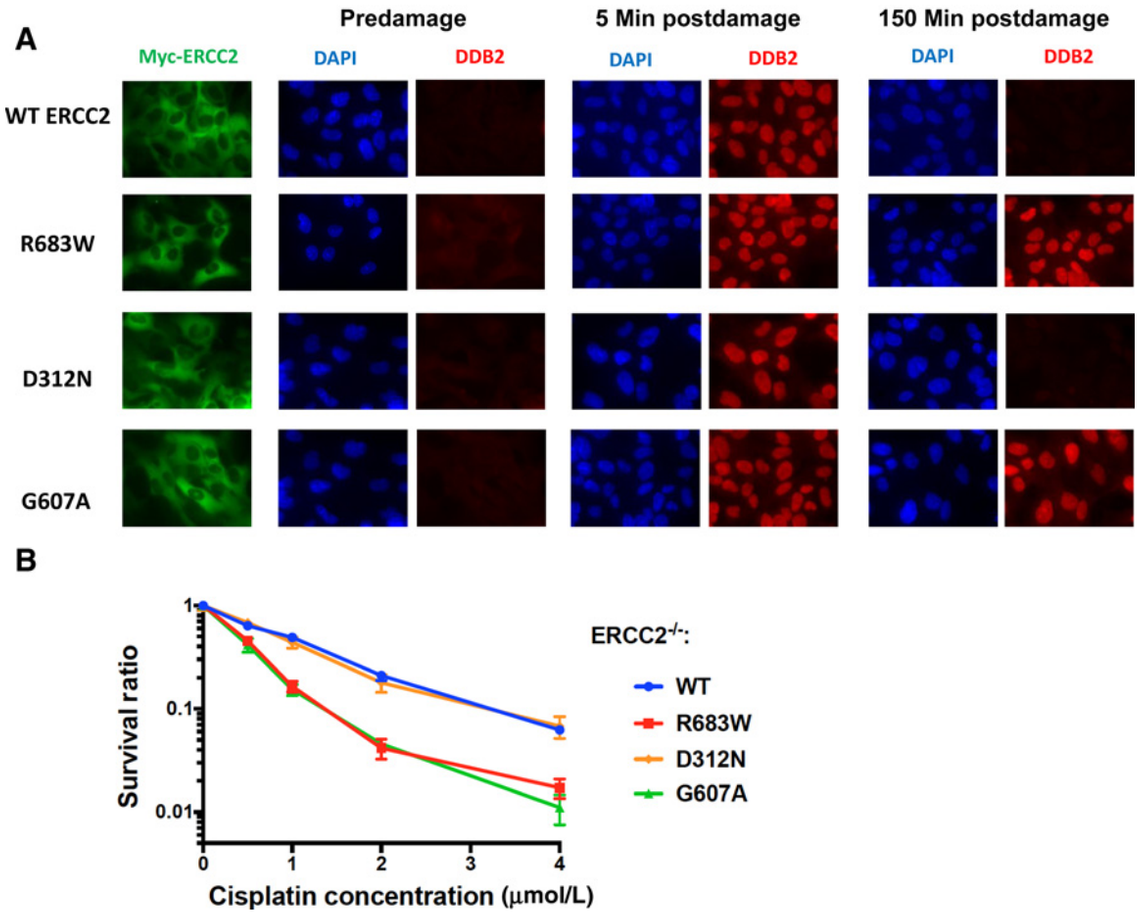

Figure 2.

UV and cisplatin sensitivity assays identify functionally deleterious *ERCC2* mutations. **A,** WT or mutant *ERCC2*-complemented cells were plated on 24-well glass slides and treated with UV irradiation. At 5 or 150 minutes following UV exposure, cells were fixed and treated with FLAG-tagged DDB2 proteoprobe ("Materials and Methods"). DDB2 proteoprobe binding to (6,4)-photoproducts is visualized using an anti-FLAG antibody (red). *ERCC2* expression is confirmed using an anti–Myc-*ERCC2* antibody (green). Nuclei are stained with DAPI (blue). R683W is a common germline pathogenic allele (33), D312N is a common nonpathogenic germline allele (34), and G607A is a mutation identified in cisplatin-responsive tumor. **B,** Cisplatin sensitivity curves for WT and mutant *ERCC2*-complemented cell lines.

ERCC2 mutations across the *ERCC2* gene. To do this, we identified all *ERCC2* coding mutations in a pooled cohort of >1,500 prospectively and retrospectively collected bladder tumors including the TCGA cohort and several single institution cohorts (Supplementary Table S1). The majority of observed *ERCC2* alterations were missense mutations, and although mutations were identified across the entire *ERCC2* gene, some positions such as Asn238 and Thr484 were mutated in multiple tumors (Fig. 1B; ref. 3). An examination of 24,592 sequenced tumors identified 9 recurrent point mutations within *ERCC2* using a published algorithm to identify hotspot mutations within genes (http://www.cancerhotspots.org/; ref. 3); however, the majority of detected alterations are of unclear functional significance.

Functional ERCC2 profiling using a novel NER assay

To understand the functional landscape of *ERCC2* mutations in MIBC, we sought to test the impact of all mutations observed across a series of MIBC cohorts and to correlate functional data with available clinical information. In addition to 98 MIBC cases from the DFCI/MSK and FCCC cohorts, we also identified all *ERCC2* mutations from TCGA bladder cancer cohort (21). Unlike the DFCI/MSK and FCCC cohorts, patients in the TCGA cohort were not routinely treated with neoadjuvant cisplatin-based chemotherapy. In total, 37 *ERCC2* mutations at 23 amino acid positions were identified across the 3 cohorts (Table 1; Supplementary Table S2). Many of these mutations have also been identified by prospective sequencing efforts at our institutions (Fig. 1).

To test the impact of each *ERCC2* mutation on NER capacity, we developed a novel fluorescence-based microscopy assay (19). The assay utilizes a purified DDB2 (damage-specific DNA-binding protein 2) proteoprobe that binds tightly and specifically to UV-induced (6,4)-photoproducts (Materials and Methods; ref. 12). Unlike DNA repair assays that measure cell survival following DNA damage and thus can take multiple days to perform, the DDB2 proteoprobe assay directly monitors DNA repair and can be completed in 2.5 hours. Immediately following UV exposure, DDB2 foci form at sites of UV-induced

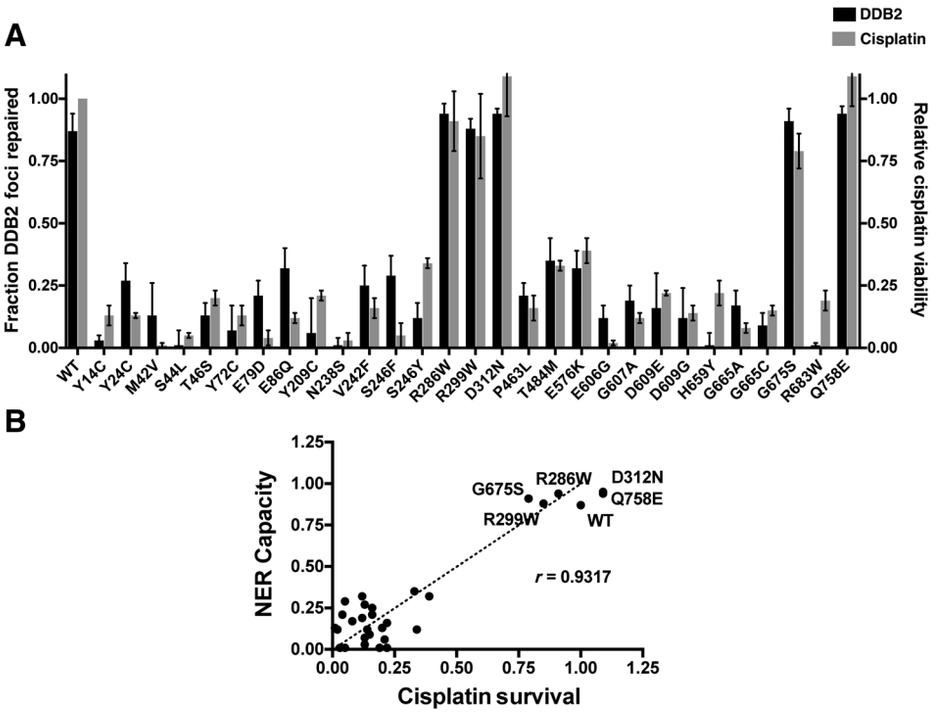

Figure 3.
Summary of UV and cisplatin sensitivity for *ERCC2* mutations across three clinical cohorts. **A,** Black bars show the fraction of DDB2 foci repaired at 150 minutes, and gray bars show cell viability in 2 μmol/L cisplatin relative to WT *ERCC2*. The majority of *ERCC2* mutations confer UV and cisplatin sensitivity; however, a subset of mutations has sensitivity profiles similar to WT *ERCC2*. **B,** There was strong correlation between UV and cisplatin sensitivity ($P < 0.001$).

(6,4)-photoproducts. In cells with intact NER, DDB2 foci are resolved over 2.5 hours as DNA damage is repaired, whereas foci persist in cells with impaired NER function (Fig. 2A; Supplementary Fig. S2).

We used the DDB2 proteoprobe assay to test all *ERCC2* mutations identified across the 3 MIBC cohorts. Each *ERCC2* mutation was expressed in an *ERCC2*-deficient fibroblast cell line derived from a patient with xeroderma pigmentosum, and the ability of each *ERCC2* mutation to rescue the UV sensitivity of the xeroderma pigmentosum cell line was quantified (Fig. 2A; Supplementary Table S2). Twenty-three of the 26 clinically observed *ERCC2* mutations failed to rescue UV sensitivity of the *ERCC2*-deficient cell line, suggesting that the mutations confer loss of cellular NER function (Fig. 3). To validate findings from the DDB2 proteoprobe assay, we also measured cisplatin sensitivity of each *ERCC2*-mutant–expressing cell line, and results from the DDB2 and cisplatin assays were strongly correlated ($P < 0.001$; Figs. 2B and 3).

We also tested the impact of *ERCC2* mutations on sensitivity to other agents commonly used to treat bladder cancer (Supplementary Fig. S3). *ERCC2*-mutant–expressing cell lines also displayed increased sensitivity to carboplatin, which creates intrastrand platinum-containing adducts that are substrates for the NER pathway. However, no differences in sensitivity to doxorubicin [a double-strand break (DSB)–inducing agent], ionizing radiation, or rucaparib, a PARP inhibitor, were noted among *ERCC2* WT- and mutant-complemented cell lines.

Most of the *ERCC2* mutations identified in tumors were located within or adjacent to conserved helicase motifs (Fig. 4). These helicase motifs are located within the two helicase domains of the ERCC2 protein (HD1 and HD2), which couple ATP hydrolysis with DNA duplex unwinding. Thirty-four of the 37 *ERCC2* mutations (20/23 amino acid positions) were located within HD1 or HD2, and in all but one case (G675S), the helicase domain mutation resulted in loss of NER function. G675 is near the 3′ end of HD2 and is located on the surface of the protein, possibly explaining why a mutation at this site is not associated with loss of NER capacity. The recent update of the TCGA bladder cancer cohort includes eight additional *ERCC2* missense mutation sites, all of which are located with the helicase domains and are therefore predicted to confer NER deficiency (22).

In addition to the helicase domains, *ERCC2* also possesses a unique ARCH domain that serves as a binding site for *ERCC2*-interacting proteins (23). Only 2 mutations in the ARCH domain were observed, but in each case, expression of the ARCH domain mutant was sufficient to rescue cisplatin and UV sensitivity of the *ERCC2*-deficient cell line, suggesting that these mutations do not disrupt NER-mediated DNA repair (Fig. 4). In addition, one mutation at the C-terminus of the ERCC2 protein (Q758E) was also not associated with loss of NER function.

ERCC2 functional status correlates with clinical outcomes

Clinical cisplatin response was available for all patients from the DFCI/MSK and FCCC cohorts. Across these two cohorts, the *ERCC2* mutation frequency was 38% in cisplatin responders versus 6% in cisplatin nonresponders (17/45 vs. 3/53, $P < 0.0001$, Fisher exact test). In each of the 17 cisplatin-responsive *ERCC2*-mutant cases, a functionally deleterious helicase domain mutation was present (Fig. 4). In one case, the deleterious helicase domain mutation (G665C) was accompanied by a nondeleterious ARCH domain mutation (R299W).

Three *ERCC2* mutations were identified in patients who did not achieve a complete response to cisplatin: S44L and S246F from the FCCC cohort and E86Q from the DFCI/MSK cohort.

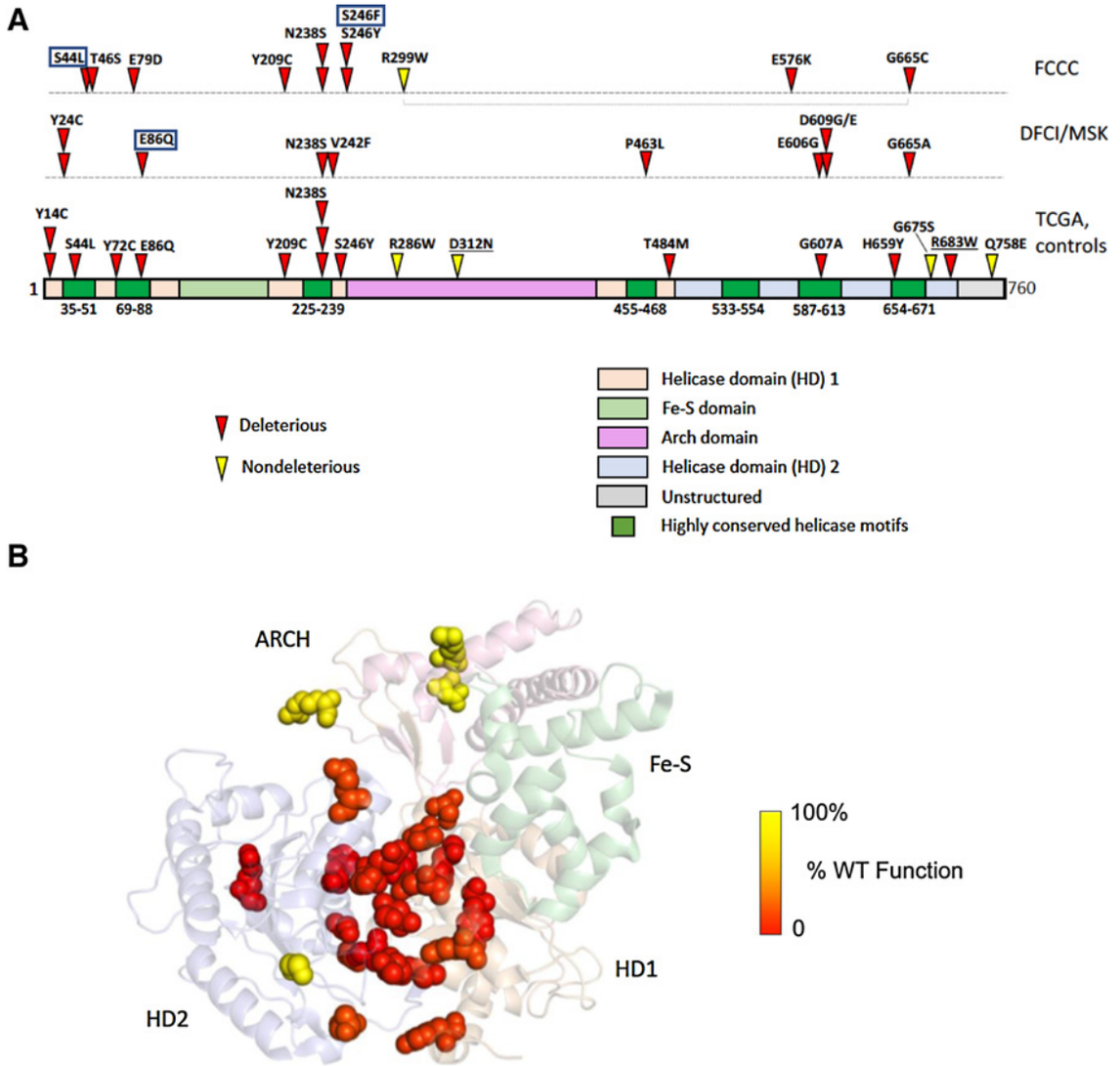

Figure 4.

Distribution and functional effects of clinically observed *ERCC2* mutations. **A,** Location of somatic *ERCC2* mutations across three clinical cohorts. Mutants that fail to rescue UV and cisplatin sensitivity (<35% WT activity) are shown in red. All other mutants had activity ≥85% of WT *ERCC2* and are shown in yellow. Clinical cisplatin response data were available for the DFCI/MSK and FCCC cohorts, and the three *ERCC2* mutations identified in cisplatin nonresponders are highlighted in boxes. D312N (underlined) is a common nonpathogenic germline allele in the general population, whereas R683W (underlined) is a common pathogenic germline allele in patients with xeroderma pigmentosum. **B,** Location of clinically observed somatic mutations in the *ERCC2* protein (PDB ID: 5IVW). Deleterious mutations (red) cluster at the interface between helicase domains, whereas nondeleterious mutations (yellow) reside in nonhelicase domains or are on the surface of the protein. Q758 was not ordered in the crystal structure and is therefore not shown.

All three mutations were located within one of the helicase domains, and functional analysis revealed that none were able to rescue cisplatin or UV sensitivity (Fig. 4; Supplementary Fig. S4). The S44L mutation was clonal and was identified in the pretreatment biopsy from a patient with clinical stage T3 MIBC who received 3 cycles of accelerated MVAC (methotrexate, vinblastine, doxorubicin, and cisplatin). Pathologic examination of the cystectomy specimen revealed residual T3aN0 disease; however, the patient remains disease-free more than 3 years following cystectomy. The S246F mutation was also clonal and was identified in the pretreatment biopsy from a patient treated with accelerated MVAC. In this case, clinical staging at diagnosis showed T4a disease with postchemotherapy downstaging to T2a, and the patient remains disease-free with nearly 2 years of follow-up. In both cases, posttreatment tumor was not available for genomic analysis, so it is unclear whether the *ERCC2* mutation was present in the residual tumor. It is possible that all *ERCC2*-mutant tumors cells were eradicated by chemotherapy and the residual (cisplatin-resistant) tumor was comprised of one or more clones with WT *ERCC2*. Alternatively, it is possible that the *ERCC2*-mutant tumor harbored concurrent cisplatin resistance mechanisms

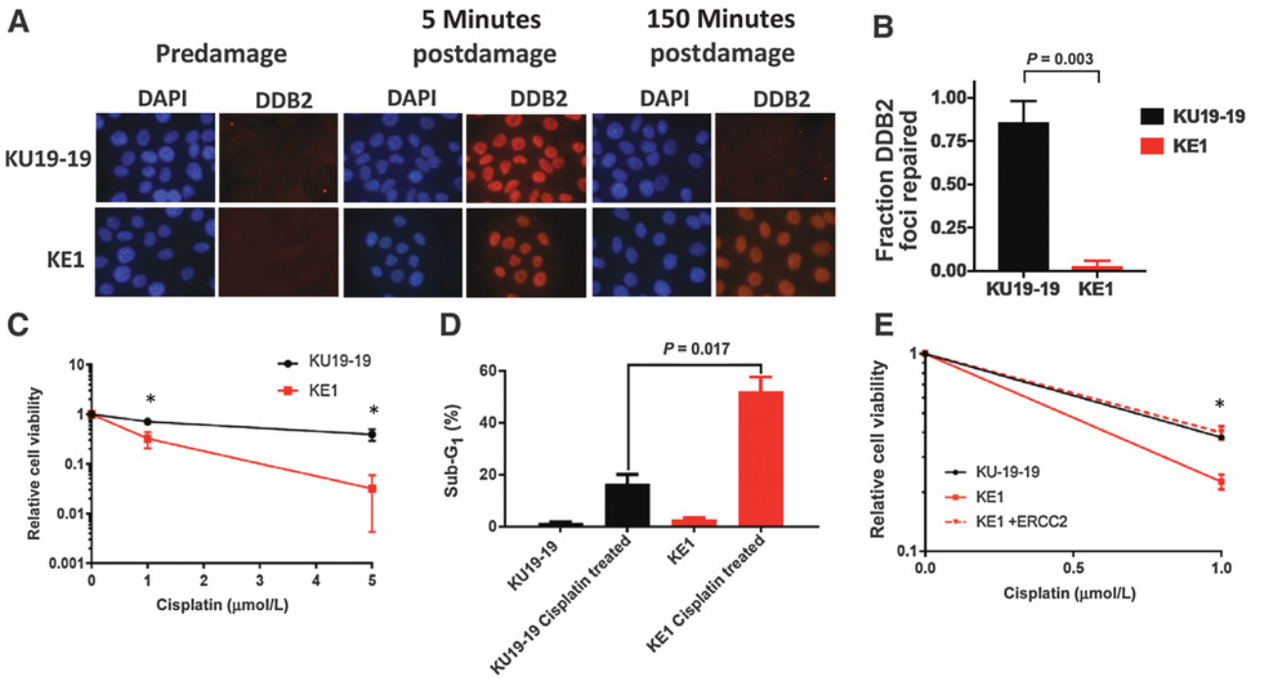

Figure 5.

An *ERCC2* mutation confers NER deficiency and cisplatin sensitivity in a bladder cancer cell line. **A,** The DDB2 proteoprobe assay was performed on the bladder cancer cell lines KU19-19 (WT *ERCC2*) and KE1, a cell line derived from KU19-19 that has an *ERCC2* M483_T484 in-frame deletion ("Materials and Methods"; Supplementary Fig. S5). **B,** KU19-19 cells efficiently repair UV-induced DNA damage, whereas damage persists in KE1 cells ($P = 0.003$). **C,** KE1 cells also display increased cisplatin sensitivity compared with the parental KU19-19 cell line ($P = 0.02$). **D,** Cell-cycle profiles of KU19-19 and KE1 cell lines before and after cisplatin treatment. The KE1 cell line has a significantly higher sub-G_1 fraction following cisplatin treatment than the KU19-19 cell line ($P = 0.017$). **E,** The cisplatin sensitivity of KE1 cells can be rescued by reexpression of WT *ERCC2* ($P = 0.03$ for KE1 vs. KE1 + WT *ERCC2*).

that were sufficient to overcome the sensitizing effect of a deleterious *ERCC2* mutation.

The third *ERCC2* mutation identified in a cisplatin nonresponder was an E86Q mutation in a patient diagnosed with clinical stage T2 disease and treated with gemcitabine and cisplatin. Cystectomy revealed a T3N0 tumor, and the patient developed recurrent disease less than one year following cystectomy. The E86Q mutation was not initially identified in the pretreatment sample by the standard mutation-calling pipeline; however, analysis of the posttreatment (cisplatin-resistant) tumor revealed the E86Q mutation in 3 of 14 reads, and subsequent directed manual review of the pretreatment sample identified the E86Q mutation in 1 of 7 reads (Supplementary Fig. S1). Other mutations were also shared between the pre- and posttreatment tumors (Supplementary Fig. S5), confirming that the tumors were phylogenetically related. In this case, co-occurring cisplatin resistance features may have overcome the effect of the deleterious *ERCC2* mutation.

An ERCC2 mutation abrogates NER activity and increases sensitivity to DNA-damaging agents in a bladder cancer preclinical model

Although nearly all tested *ERCC2* mutations were unable to support normal cellular NER or rescue the cisplatin sensitivity of an *ERCC2*-deficient fibroblast-derived cell line, the effect of *ERCC2* mutations on NER capacity and cisplatin sensitivity in bladder cancer cells is unknown. To determine whether an *ERCC2* mutation is sufficient to drive cisplatin sensitivity in a bladder cancer context, we used Clustered Regularly Interspaced Short Palindromic Repeats (CRISPR)/Cas9 technology to introduce an *ERCC2* mutation in the high-grade bladder transitional cell carcinoma cell line KU19-19 (24). We infected the WT *ERCC2* parental KU19-19 cell line with a CRISPR/Cas9 lentivirus targeting residue T484 of *ERCC2*, the site of a mutation (T484M) observed in the TCGA cohort. The KU19-19 cell line is triploid at the *ERCC2* locus, and we recovered a mutant cell line (KE1) harboring nonsense mutations in two copies and an M483_T484 in-frame deletion in the third copy (Supplementary Fig. S6).

To determine the effect of the *ERCC2* mutation on NER activity, we performed the DDB2 proteoprobe assay on the parental KU19-19 and the *ERCC2*-mutant KE1 cell lines (Fig. 5A; Supplementary Fig. S7). Similar to the *ERCC2* mutants that failed to rescue UV sensitivity in the xeroderma pigmentosum cell line, we observed persistence of DDB2 foci at 2.5 hours following UV exposure in the *ERCC2*-mutant KE1 cell line. In contrast, the WT *ERCC2* KU19-19 parental line efficiently repaired UV-induced DNA damage ($P = 0.003$; Fig. 5B).

We next compared the cisplatin sensitivity profiles of the KU19-19 and *ERCC2*-mutant KE1 cell lines and found that the presence of the *ERCC2* mutation led to a significant increase in cisplatin sensitivity ($P = 0.02$; Fig. 5C). Cell-cycle analysis revealed a higher sub-G_1 fraction following cisplatin exposure in KE1 cells compared with KU19-19 cells,

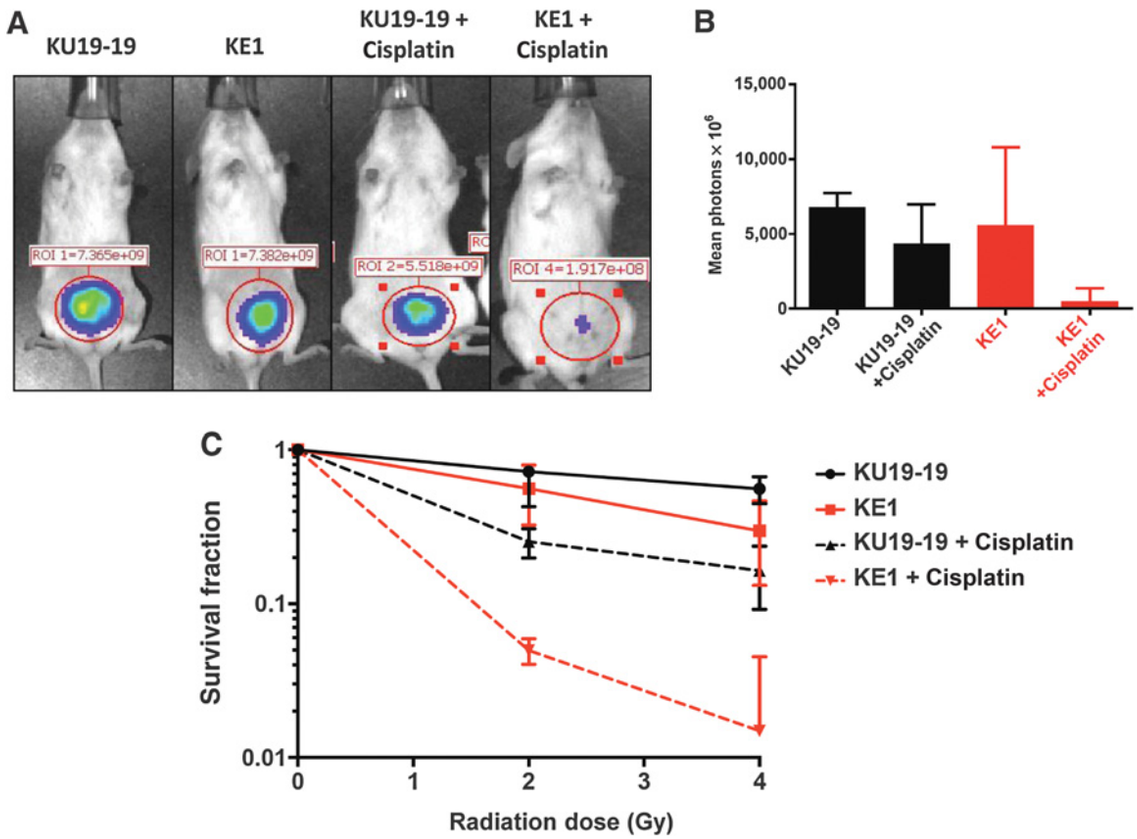

Figure 6.

An *ERCC2* mutation confers cisplatin sensitivity in an orthotopic bladder cancer model but does not sensitize to ionizing radiation. **A,** KU19-19 (*ERCC2* WT) or KE1 (*ERCC2* mutant) cells were implanted into the bladders of nude mice (4 mice/cell line), and mice were treated with cisplatin or saline. Representative images from posttreatment day 14 are shown. **B,** There was no difference in tumor size between the KU19-19 and KE1 models in the absence of cisplatin; however, KE1 tumors shrink markedly following cisplatin treatment. **C,** No significant difference in clonogenic survival following ionizing radiation was noted between the KU19-19 and KE1 cell lines (solid lines). However, there was a significant difference in survival following combined treatment with cisplatin and ionizing radiation (dashed lines; $P = 0.05$ for interaction between cisplatin and radiation in KU19-19 vs. KE1).

consistent with increased cell death ($P = 0.017$; Fig. 5D). Cisplatin sensitivity of the KE1 cell line could be rescued by reexpression of WT *ERCC2* ($P = 0.03$ for KE1 vs. KE1 + WT *ERCC2*; Fig. 5E).

We next measured the effect of the *ERCC2* mutation on cisplatin sensitivity *in vivo*. Luciferase-labeled KU19-19 or KE1 cells were injected into the bladders of immunodeficient mice to establish orthotopic tumor models, and animals were subsequently treated with cisplatin or saline (Supplementary Methods). Whereas there was no difference in growth of the KE1 versus KU19-19 tumors in the absence of cisplatin, near complete resolution of KE1 tumors was noted following cisplatin treatment, while KU19-19 tumors showed minimal response (Fig. 6A and B).

DNA-damaging agents are commonly used in the treatment of MIBC, and cisplatin can be combined with radiation in a bladder-sparing trimodality therapy approach (25–27). To determine the effect of an *ERCC2* mutation on sensitivity to combination DNA-damaging therapy, we compared the sensitivity of the KU19-19 and KE1 cell lines to radiation with or without concurrent cisplatin. Ionizing radiation causes primarily DNA DSBs, and there was not a significant difference in radiation sensitivity between the KU19-19 and KE1 cell lines (Fig. 6C). However, KE1 cells were significantly more sensitivity when cisplatin was combined with radiation ($P = 0.05$ for interaction between cisplatin and radiation in KU19-19 vs. KE1), consistent with *ERCC2*'s role in NER-mediated repair of cisplatin-induced intrastrand DNA adducts. No difference in sensitivity to the PARP inhibitor olaparib, which primarily targets DSB repair–deficient cells, was observed (Supplementary Fig. S8).

Discussion

DNA repair pathway alterations can drive tumor behavior and therapy response. In addition, germline mutations in DNA repair genes cause a variety of inherited diseases and can be associated with increased cancer risk. However, for many DNA repair genes, the functional landscape of missense mutations has not been fully characterized, resulting in an inability to reliably predict clinical impact. Furthermore, studying the effects of DNA repair pathway alterations in relevant tumor contexts is challenging, yet is essential to understand the impact of mutations on tumor biology and therapy response.

Here, we functionally profile the effects of *ERCC2* missense mutations observed in muscle-invasive bladder tumors and correlate our findings with clinical outcomes. Using a novel assay that allows us to directly measure NER proficiency, we find that nearly all clinically observed *ERCC2* missense mutations were unable to support normal cellular NER. Correspondingly, the *ERCC2* mutations also resulted in increased sensitivity to agents such as cisplatin and carboplatin that create DNA adducts normally repaired by the NER pathway, but not to agents such as doxorubicin or ionizing radiation that primarily cause DNA DSBs, or to PARP inhibitors, which target cells with defective DSB repair.

In order to determine whether an *ERCC2* mutation is sufficient to drive cisplatin sensitivity in bladder tumors, we used CRISPR/Cas9 technology to create a bladder cancer cell line harboring a mutation at the endogenous *ERCC2* locus. Given its role in general transcription (as a core subunit of the TFIIH complex), *ERCC2* is an essential gene and complete *ERCC2* loss is not tolerated by cells. The *ERCC2*-mutant KE1 cell line harbors an *ERCC2* M483_T484 in-frame deletion, fails to repair UV-induced DNA damage, and shows increased sensitivity to cisplatin both *in vitro* and *in vivo*. Similarly, a T484M missense mutation that has been identified in multiple retrospective and prospective cohorts did not rescue UV or cisplatin in our xeroderma pigmentosum complementation assays. Taken together, these results suggest that introducing a mutation at a common site of clinically observed mutations in *ERCC2* is sufficient to confer cisplatin sensitivity in a bladder cancer context.

Finally, we correlated our functional findings with available clinical data. All patients in the DFCI/MSK and FCCC cohorts received neoadjuvant cisplatin-based chemotherapy, and nearly all patients (17/20, 85%) with an *ERCC2*-mutant tumor in these cohorts had no evidence of residual MIBC at the time of cystectomy. This response rate of 85% compares favorably with the approximately 35% complete response rate observed in unselected populations (4, 5). In both the DFCI/MSK and FCCC cohorts, patients with *ERCC2*-mutated tumors lived significantly longer than patients with WT *ERCC2* tumors (8), consistent with the known association between complete response and overall survival observed in other MIBC cohorts (28). Our functional analysis revealed that nearly all of these clinically observed *ERCC2* mutations were unable to perform NER and were also associated with increased cisplatin sensitivity, providing a mechanistic basis for the role for *ERCC2* mutations as a predictive biomarker of cisplatin sensitivity in MIBC. *ERCC2* mutations were not associated with improved survival in the TCGA cohort (in which patients did not receive neoadjuvant chemotherapy), suggesting that *ERCC2* is a stronger predictive than prognostic biomarker (Supplementary Fig. S9).

In three cases, the presence of an *ERCC2* mutation was not associated with complete response to cisplatin. Functional assessment revealed that each of these mutations conferred NER deficiency and cisplatin sensitivity *in vitro*, and in each case, mutation of the same amino acid was associated with complete cisplatin response in one or more other patients. Therefore, a deleterious *ERCC2* mutation does not appear to be sufficient to drive complete cisplatin response in all cases. In two of these cases, the posttreatment tumor was not available for analysis, so it is possible that the residual tumor is comprised of one or more WT *ERCC2* clones that persisted through cisplatin-based chemotherapy. Interestingly, despite an incomplete response, both of these patients remain disease free with several years of follow-up. In the third *ERCC2*-mutant nonresponder, the posttreatment tumor was analyzed and was found to harbor the same *ERCC2* mutation identified in the pretreatment biopsy. In this case, a compensatory cisplatin resistance mechanism such as upregulation of an alternative DNA repair pathway, a damage tolerance pathway, or a drug efflux pump may be responsible for mediating cisplatin resistance (29). Further work aimed at understanding the molecular underpinnings of incomplete response in these outlier cases may provide broader insights regarding mechanisms of resistance to DNA-damaging therapies. Pretreatment bladder tumors collected through the recently completed SWOG1314 study, which seeks to validate RNA expression–based predictive biomarkers of neoadjuvant chemosensitivity in MIBC, will be analyzed using a multi-platform approach and should provide additional data on genomic predictors of response to platinum-based chemotherapy.

As prospective sequencing efforts continue to become integrated into clinical practice, predicting the functional relevance and determining the clinical actionability of novel mutations in cancer genes remains a significant challenge. DNA repair deficiency is an important predictive biomarker in several clinical contexts, and DNA repair pathway alterations have recently been associated with increased sensitivity to immune checkpoint blockade in bladder cancer and other tumor types (10, 11, 30), providing further motivation to characterize the functional impact of DNA repair variants. Development and clinical integration of rapid, reliable, and cost-effective functional assays represents one solution to this challenge and may be particularly relevant for DNA damage response (DDR) genes such as *BRCA1/2* in which variants of uncertain significance are commonly observed.

Here, we used genomic and functional approaches to understand the consequences of mutations in *ERCC2*, an emerging cancer gene (3). We created a robust assay to measure the functional impact of *ERCC2* mutations and identified a strong correlation among helicase domain mutations, NER pathway dysfunction, and clinical cisplatin response. Together, these data establish a role for *ERCC2* helicase domain mutations as an MIBC biomarker that may be useful in guiding therapy decisions (31). Indeed, *ERCC2* mutational status has already been incorporated as a prospective biomarker in risk-adapted MIBC clinical trials. An Alliance for Clinical Trials in Oncology study (A031701) as well as a separate multi-institution study (NCT02710734) will each offer chemotherapy alone without radical cystectomy for patients whose pretreatment tumor specimen contains prespecified DDR gene alterations and who achieve a complete clinical response to cisplatin-based therapy (32). A Hoosier Cancer Research Network trial (NCT03558087) investigating neoadjuvant chemoimmunotherapy also includes selective biomarker-based bladder-sparing for patients with tumor mutations in *ERCC2* or other DDR genes.

Disclosure of Potential Conflicts of Interest

J. Bellmunt is a consultant/advisory board member for Merck, Pfizer, AstraZeneca, Pierre Fabre, and Roche. D.F. Bajorin reports receiving commercial research grants from Bristol-Myers Squibb, Merck, and Novartis; reports receiving speakers bureau honoraria from Merck; and is a consultant/advisory board member for Merck, Genentech, and Pfizer. J.E. Rosenberg is listed as a co-inventor on a patent regarding ERCC2 mutation to select patients for platinum-

based chemotherapy that is owned by Memorial Sloan Kettering Cancer Center. E.M. Van Allen reports receiving commercial research grants from Novartis and Bristol-Myers Squibb; reports receiving speakers bureau honoraria from Illumina; holds ownership interest (including patents) in Genome Medical, Synapse, and Tango Therapeutics; and is a consultant/advisory board member for Genome Medical, Invitae, and Tango Therapeutics. K.M. Mouw is a consultant/advisory board member for EMD Serono and Pfizer. No potential conflicts of interest were disclosed by the other authors.

Authors' Contributions

Conception and design: Q. Li, D. Liu, S.P. Gao, D.B. Solit, J.E. Rosenberg, A.D. D'Andrea, E.M. Van Allen, G. Iyer, K.W. Mouw

Development of methodology: Q. Li, A.W. Damish, Z. Frazier, D. Liu, H. Zhao, S.P. Gao, J. Ma, J. Bellmunt, J.-B. Lazaro, D.B. Solit, E.M. Van Allen, K.W. Mouw

Acquisition of data (provided animals, acquired and managed patients, provided facilities, etc.): Q. Li, A.W. Damish, Z. Frazier, A. Bell, H. Zhao, E.J. Jordan, S.P. Gao, J. Ma, J. Bellmunt, E.R. Plimack, D.B. Solit, D. Bajorin, N. Riaz, E.M. Van Allen, G. Iyer, K.W. Mouw

Analysis and interpretation of data (e.g., statistical analysis, biostatistics, computational analysis): Q. Li, Z. Frazier, D. Liu, E. Reznichenko, A. Kamburov, A. Bell, S.P. Gao, J. Ma, J. Bellmunt, D.B. Solit, D. Bajorin, J.E. Rosenberg, N. Riaz, E.M. Van Allen, G. Iyer, K.W. Mouw

Writing, review, and/or revision of the manuscript: Q. Li, Z. Frazier, D. Liu, E. Reznichenko, P.H. Abbosh, J. Bellmunt, E.R. Plimack, D.B. Solit, D. Bajorin, J.E. Rosenberg, A.D. D'Andrea, N. Riaz, E.M. Van Allen, G. Iyer, K.W. Mouw

Administrative, technical, or material support (i.e., reporting or organizing data, constructing databases): Q. Li, J.-B. Lazaro, D.B. Solit

Study supervision: S.P. Gao, J. Bellmunt, D.B. Solit, J.E. Rosenberg, G. Iyer, K.W. Mouw

Acknowledgments

Q. Li was supported in part by an NIH T32 training grant (CA082088). J.E. Rosenberg, G. Iyer, E.M. Van Allen, and K.W. Mouw were funded by the Starr Cancer Consortium. J.E. Rosenberg, G. Iyer, and D.B. Solit were funded by an NIH P30 grant (CA008748) to Memorial Sloan Kettering Cancer Center, and G. Iyer was also funded through a Geoffrey Beene Cancer Research Center grant. P.H. Abbosh is supported by an NIH R21 award (R21CA218976). E.M. Van Allen was funded by the Damon Runyon Cancer Research Foundation. A.D. D'Andrea and K.W. Mouw were funded by the Ludwig Center at Harvard. K.W. Mouw was also funded by the NCI (1K08CA219504), the Burroughs-Wellcome Fund, and the Bladder Cancer Advocacy Network (BCAN).

The costs of publication of this article were defrayed in part by the payment of page charges. This article must therefore be hereby marked *advertisement* in accordance with 18 U.S.C. Section 1734 solely to indicate this fact.

Received April 2, 2018; revised June 4, 2018; accepted July 2, 2018; published first July 6, 2018.

References

1. Garraway LA, Lander ES. Lessons from the cancer genome. Cell 2013; 153:17–37.
2. Van Allen EM, Wagle N, Stojanov P, Perrin DL, Cibulskis K, Marlow S, et al. Whole-exome sequencing and clinical interpretation of formalin-fixed, paraffin-embedded tumor samples to guide precision cancer medicine. Nat Med 2014;20:682–8.
3. Chang MT, Bhattarai TS, Schram AM, Bielski CM, Donoghue MTA, Jonsson P, et al. Accelerating discovery of functional mutant alleles in cancer. Cancer Discov 2018;8:174–83.
4. Neoadjuvant cisplatin, methotrexate, and vinblastine chemotherapy for muscle-invasive bladder cancer: a randomised controlled trial. International collaboration of trialists. Lancet 1999;354:533–40.
5. Grossman HB, Natale RB, Tangen CM, Speights VO, Vogelzang NJ, Trump DL, et al. Neoadjuvant chemotherapy plus cystectomy compared with cystectomy alone for locally advanced bladder cancer. N Engl J Med 2003;349:859–66.
6. Porter MP, Kerrigan MC, Donato BM, Ramsey SD. Patterns of use of systemic chemotherapy for Medicare beneficiaries with urothelial bladder cancer. Urol Oncol 2011;29:252–8.
7. Van Allen EM, Mouw KW, Kim P, Iyer G, Wagle N, Al-Ahmadie H, et al. Somatic ERCC2 mutations correlate with cisplatin sensitivity in muscle-invasive urothelial carcinoma. Cancer Discov 2014;4:1140–53.
8. Liu D, Plimack ER, Hoffman-Censits J, Garraway LA, Bellmunt J, Van Allen E, et al. Clinical validation of chemotherapy response biomarker ERCC2 in muscle-invasive urothelial bladder carcinoma. JAMA Oncol 2016;2: 1094–6.
9. Teo MY, Bambury R, Zabor EC, Jordan EJ, Al-Ahmadie HA, Boyd M, et al. DNA damage response and repair gene alterations are associated with improved survival in patients with platinum-treated advanced urothelial carcinoma. Clin Cancer Res 2017;23:3610–8.
10. Galsky MD, Wang H, Hahn NM, Twardowski P, Pal SK, Albany C, et al. Phase 2 trial of gemcitabine, cisplatin, plus ipilimumab in patients with metastatic urothelial cancer and impact of DNA damage response gene mutations on outcomes. Eur Urol 2018;73:715–9.
11. Teo MY, Seier K, Ostrovnaya I, Regazzi AM, Kania BE, Moran MM, et al. Alterations in DNA damage response and repair genes as potential marker of clinical benefit from PD1/PDL1 blockade in advanced urothelial cancers. J Clin Oncol 2018;36:1685–94.
12. Marteijn JA, Lans H, Vermeulen W, Hoeijmakers JH. Understanding nucleotide excision repair and its roles in cancer and ageing. Nat Rev Mol Cell Biol 2014;15:465–81.
13. Guidugli L, Carreira A, Caputo SM, Ehlen A, Galli A, Monteiro AN, et al. Functional assays for analysis of variants of uncertain significance in BRCA2. Hum Mutat 2014;35:151–64.
14. O'Connor M.J. Targeting the DNA damage response in cancer. Mol Cell 2015;60:547–60.
15. Zehir A, Benayed R, Shah RH, Syed A, Middha S, Kim HR, et al. Mutational landscape of metastatic cancer revealed from prospective clinical sequencing of 10,000 patients. Nat Med 2017;23:703–13.
16. Brastianos PK, Carter SL, Santagata S, Cahill DP, Taylor-Weiner A, Jones RT, et al. Genomic characterization of brain metastases reveals branched evolution and potential therapeutic targets. Cancer Discov 2015;5: 1164–77.
17. Carter SL, Cibulskis K, Helman E, McKenna A, Shen H, Zack T, et al. Absolute quantification of somatic DNA alterations in human cancer. Nat Biotechnol 2012;30:413–21.
18. Sanjana NE, Shalem O, Zhang F. Improved vectors and genome-wide libraries for CRISPR screening. Nat Methods 2014;11:783–84.
19. Dreze M, Calkins AS, Galicza J, Echelman DJ, Schnorenberg MR, Fell GL, et al. Monitoring repair of UV-induced 6–4-photoproducts with a purified DDB2 protein complex. PLoS One 2014;9:e85896.
20. Ponomarev V, Doubrovin M, Serganova I, Beresten T, Vider J, Shavrin A, et al. Cytoplasmically retargeted HSV1-tk/GFP reporter gene mutants for optimization of noninvasive molecular-genetic imaging. Neoplasia 2003;5:245–54.
21. The Cancer Genome Atlas Research Network. Comprehensive molecular characterization of urothelial bladder carcinoma. Nature 2014;507: 315–22.
22. Robertson AG, Kim J, Al-Ahmadie H, Bellmunt J, Guo G, Cherniack AD, et al. Comprehensive molecular characterization of muscle-invasive bladder cancer. Cell 2017;171:540–56.
23. Abdulrahman W, Iltis I, Radu L, Braun C, Maglott-Roth A, Giraudon C, et al. ARCH domain of XPD, an anchoring platform for CAK that conditions TFIIH DNA repair and transcription activities. Proc Natl Acad Sci U S A 2013;110:E633–42.
24. Tachibana M, Miyakawa A, Tazaki H, Nakamura K, Kubo A, Hata J, et al. Autocrine growth of transitional cell carcinoma of the bladder induced by granulocyte-colony stimulating factor. Cancer Res 1995;55:3438–43.
25. Ploussard G, Daneshmand S, Efstathiou JA, Herr HW, James ND, Rodel CM, et al. Critical analysis of bladder sparing with trimodal therapy in muscle-invasive bladder cancer: a systematic review. Eur Urol 2014;66: 120–37.

26. Giacalone NJ, Shipley WU, Clayman RH, Niemierko A, Drumm M, Heney NM, et al. Long-term outcomes after bladder-preserving tri-modality therapy for patients with muscle-invasive bladder cancer: an updated analysis of the Massachusetts General Hospital experience. Eur Urol 2017;71:952–60.
27. Mak RH, Hunt D, Shipley WU, Efstathiou JA, Tester WJ, Hagan MP, et al. Long-term outcomes in patients with muscle-invasive bladder cancer after selective bladder-preserving combined-modality therapy: a pooled analysis of radiation therapy oncology group protocols 8802; 8903; 9506; 9706; 9906; and 0233. J Clin Oncol 2014;32:3801–9.
28. Sonpavde G, Goldman BH, Speights VO, Lerner SP, Wood DP, Vogelzang NJ, et al. Quality of pathologic response and surgery correlate with survival for patients with completely resected bladder cancer after neoadjuvant chemotherapy. Cancer 2009;115:4104–9.
29. Galluzzi L, Senovilla L, Vitale I, Michels J, Martins I, Kepp O, et al. Molecular mechanisms of cisplatin resistance. Oncogene 2012;31:1869–83.
30. Le DT, Uram JN, Wang H, Bartlett BR, Kemberling H, Eyring AD, et al. PD-1 blockade in tumors with mismatch-repair deficiency. N Engl J Med 2015;372:2509–20.
31. Chakravarty D, Gao J, Phillips SM, Kundra R, Zhang H, Wang J, et al. OncoKB: a precision oncology knowledge base. JCO Precis Oncol 2017;2017:1–16.
32. Geynisman DM, Abbosh P, Zibelman MR, Feldman R, McConkey DJ, Hahn NM, et al. A phase II risk-adapted treatment for muscle invasive bladder cancer after neoadjuvant accelerated MVAC. J Clin Oncol 36, 2018 (suppl 6S; abstr TPS537).
33. Ueda T, Compe E, Catez P, Kraemer KH, Egly JM. Both XPD alleles contribute to the phenotype of compound heterozygote xeroderma pigmentosum patients. J Exp Med 2009;206:3031–46.
34. Lunn RM, Helzlsouer KJ, Parshad R, Umbach DM, Harris EL, Sanford KK, et al. XPD polymorphisms: effects on DNA repair proficiency. Carcinogenesis 2000;21:551–5.